Received Date : 11-Jun-2016

Revised Date : 14-Oct-2016

Accepted Date : 17-Oct-2016

Article type : Research Report

Progesterone analogue protects stressed photoreceptors via bFGF-mediated calcium influx

Alice C. Wyse-Jackson†, Sarah L. Roche†, Ana M. Ruiz-Lopez†, Jennifer N. Moloney†, Ashleigh M. Byrne†, Thomas G. Cotter†*

†Cell Development and Disease Laboratory, Biochemistry Department, Bioscience Research Institute, University College Cork, Cork, Ireland

** Corresponding Author. Email: t.cotter@ucc.ie; Address: Cell Development and Disease Laboratory, Biochemistry Department, Bioscience Research Institute, University College Cork, Cork, Ireland; Tel: +353 21 4901321; Fax: +353 21 4901382*

Running Title:

Progesterone: PGRMC1, bFGF & calcium influx

Suggested Section:

Molecular and Synaptic Mechanisms

Keywords:

Norgestrel, 661W, PGRMC1, Neuroprotection, Retina

This article has been accepted for publication and undergone full peer review but has not been through the copyediting, typesetting, pagination and proofreading process, which may lead to differences between this version and the Version of Record. Please cite this article as doi: 10.1111/ejn.13445

Abstract

Retinitis pigmentosa (RP) is a degenerative retinal disease leading to photoreceptor cell loss. In 2011, our group identified the synthetic progesterone 'Norgestrel' as a potential treatment for RP. Subsequent research showed Norgestrel to work through progesterone receptor membrane component 1 (PGRMC1) activation and upregulation of neuroprotective basic fibroblast growth factor (bFGF). Using trophic factor deprivation of 661W photoreceptor-like cells, we aimed to further elucidate the mechanism leading to Norgestrel-induced neuroprotection.

In the present manuscript, we show by flow cytometry and live-cell immunofluorescence that Norgestrel induces an increase in cytosolic calcium in both healthy and stressed 661Ws over 24h. Specific PGRMC1 inhibition by AG205 (1 μM) showed this rise to be PGRMC1-dependent, primarily utilising calcium from extracellular sources, for blockade of L-type calcium channels by verapamil (50 μM) prevented a Norgestrel-induced calcium influx in stressed cells. Calcium influx was also shown to be bFGF-dependent, for siRNA knock down of bFGF prevented Norgestrel-PGRMC1 induced changes in cytosolic calcium. Notably, we demonstrate PGRMC1-activation is necessary for Norgestrel-induced bFGF upregulation. We propose that Norgestrel protects through the following pathway: binding to and activating PGRMC1 expressed on the surface of photoreceptor cells, PGRMC1 activation drives bFGF upregulation and subsequent calcium influx. Importantly, raised intracellular calcium is critical to Norgestrel's protective efficacy, for extracellular calcium chelation by EGTA abrogates the protective effects of Norgestrel on stressed 661W cells *in vitro*.

Introduction

Retinitis pigmentosa (RP) is the name given to a group of hereditary degenerative eye disorders whereby light-sensitive photoreceptor cells are lost (Samardzija *et al.*, 2012). Several successful gene therapies have been implemented for the treatment of RP (Pang *et al.* 2008; Koch *et al.* 2012; Mookherjee *et al.* 2015), however the disease is extremely heterogeneous. Nearly 3100 mutations in 50 different genes have been reported to cause nonsyndromic RP (Daiger *et al.*, 2013). Therefore, a non-gene specific treatment for retinal neurodegenerative diseases is still highly desirable.

Progesterone signalling is coming to the forefront of many neuroprotective strategies. With proven efficacy against stroke, Alzheimer's disease and traumatic brain injury (Gonzalez Deniselle *et al.*, 2002a; 2002b; Gonzalez *et al.*, 2005; Compagnone, 2008; Espinosa-García *et al.*, 2014; Yousuf *et al.*, 2014; Qin *et al.*, 2015), evidence now also suggests a potential therapeutic role in degenerative retinal diseases (Lu *et al.*, 2008; Allen *et al.*, 2015). Certainly, a wealth of studies exist indicating that progesterone improves neuronal survival; reducing swelling, apoptosis and damaging inflammatory processes (Gonzalez Deniselle *et al.* 2002a; Lu *et al.* 2008; Garay *et al.* 2011; Allen *et al.* 2015). Indeed, our own group have shown the synthetic progestin 'Norgestrel' to be neuroprotective to stressed photoreceptors (Doonan *et al.*, 2011; Doonan & Cotter, 2012), acting through progesterone receptor membrane complex one (PGRMC1) (Wyse-Jackson *et al.*, 2016) and upregulating pro-survival growth factors (Byrne *et al.*, 2016; Wyse-Jackson & Cotter, 2016).

Progesterone signalling has been linked to changes in intracellular retinal cytosolic calcium concentrations ($[Ca^{2+}]_i$), both increased (Samadi *et al.* 2002; Koulen *et al.* 2008) and decreased (Luoma *et al.*, 2012). These fluctuations have important functional implications on survival signalling events, as calcium is a multifaceted second messenger. In terms of timing, calcium can trigger exocytosis of vesicles from synaptic terminals within microseconds. However, in order to drive gene transcription and proliferative events, calcium requires a longer signalling period: minutes to hours (Berridge *et al.*, 2003). Alternately to timing, differing cytosolic calcium concentrations will also preferentially affect signalling. For example, one paper found that intermediate levels of $[Ca^{2+}]_i$ (50-200 nM in rat hippocampal neurons) induced a long-term tolerance of ischemia. Neurons exposed to higher or lower $[Ca^{2+}]_i$ however, died upon glucose and oxygen deprivation (Bickler & Fahlman, 2004). Interestingly, protective, moderate increases in $[Ca^{2+}]_i$ increased the tolerance of subsequent larger increases in $[Ca^{2+}]_i$ (Bickler & Fahlman, 2004), previously shown to induce cell death (Sharma and Rohrer 2004; Guerin *et al.* 2011).

Time/concentration dynamics of calcium allow for heterogeneity in calcium-dependent pro-survival systems. However, upstream of these pathways is extensive machinery driving cytosolic influx. This machinery, comprised of neurotransmitters and their receptors, intracellular signalling factors and transcription factors to name a few (Pinto *et al.*, 2016), forms a diverse network of interactions. These interactions can then associate and drive a variety of different processes. In this study, we look at the potential of neuroprotective basic fibroblast growth factor (bFGF) (Désiré *et al.* 2000; O'Driscoll *et al.* 2007; O'Driscoll *et al.* 2008; Yang *et al.* 2014) to drive cytosolic calcium influx. bFGF has previously been shown to affect $[Ca^{2+}]_i$ through calcium channel modulation (Puro and Mano 1991; Rosenthal *et al.* 2005; Zamburlin *et al.* 2013). For example, bFGF-dependent calcium influx through L- and N-type voltage-dependent calcium channels stimulates neurite outgrowth *ex vivo* (Zamburlin *et al.*, 2013), driving retinal axon extension (Lom *et al.*, 1998). bFGF induced proliferation is also postulated to be calcium dependent (Puro & Mano, 1991). Consequently we hypothesised a link between bFGF-dependent neuroprotection (Doonan *et al.*, 2011; Wyse-Jackson & Cotter, 2016) and raised cytosolic calcium in stressed photoreceptors.

Clearly, the mechanisms linking progesterone-induced calcium signalling to cell survival are ill-defined. Therefore, in this study, we tested a number of hypotheses **as have been outlined in Figure 1**: Firstly, Norgestrel administration affects $[Ca^{2+}]_i$ in stressed photoreceptor cells. Secondly, this effect is PGRMC1-Norgestrel binding-dependent. Thirdly, Norgestrel acts through bFGF to affect $[Ca^{2+}]_i$. And fourthly, an altered cytosolic calcium concentration is necessary for Norgestrel-induced cell survival. Through this work, we hope to further elucidate the pro-survival pathway involved in Norgestrel's neuroprotective capabilities.

Materials and Methods

Reagents, Primers and Antibodies

Norgestrel (N2260) and dimethyl sulfoxide (DMSO) (D2650) were purchased from Sigma (Dublin, Ireland). The Ca^{2+} indicator 2,2'-((2-(2-(2-(bis(carboxymethyl)amino)-5-(2,7-difluoro-6-hydroxy-3-oxo-3H-xanthen-9-yl)phenoxy)ethoxy)-4-methylphenyl)azanediyl)diacetic acid (Fluo-4 AM) (F-14201) was supplied by Thermo Fischer (Waltham, MA, USA). PGRMC1 specific inhibitor AG205 (A1487), the ryanodine receptor antagonist dantrolene (D9175), calcium chelator EGTA (E3889) and L-type Ca^{2+} channel blocker Verapamil (V105) were all obtained from Sigma. CellTiter 96® AQueous One Solution Cell Proliferation Assay [3-(4,5-dimethylthiazol-2-yl)-5-(3-carboxymethoxyphenyl)-2-(4-sulfophenyl)-2H-tetrazolium (MTS) solution (G3580) was provided by Promega (Madison, WI, USA). Primary antibody FGF2/basic FGF, clone bFM-2 (1:200) (#05-118) from Millipore Ireland B.V. (Cork, Ireland) was used for immunofluorescence. Peroxidase-coupled secondary antibodies (Alexa Fluor-594, Alexa Fluor-488) were purchased from Invitrogen (Carlsbad, CA, USA) and Hoechst 33342 was bought from Sigma. Qiagen QuantiTect Primer assays were used in all rt-qPCR arrays **(Table 1).** FGF2 GeneSolution siRNA (#GS14173) and Allstars Negative Control siRNA (#1027280) were transfected in to cells using HiPerFect Transfection Reagent (#301705), all from Qiagen (Hilden, Germany).

Cell Culture and Treatments

Experiments were carried out using the mouse photoreceptor-derived 661W cell line. This cell line was generously provided by Dr Muayyad Al-Ubaidi (Department of Cell Biology, University of Oklahoma, Health Sciences Centre, Oklahoma City, OK, USA). Validation of this cell line was previously carried out by this group (Wyse-Jackson *et al.*, 2016) through rt-qPCR analysis for cone specific opsins (Ait-Hmyed *et al.*, 2013). This yielded a positive result confirming a cone cell phenotype. Cells were cultured in Dulbecco's Modified Eagle's medium (D6429) (Sigma) supplemented with 10% foetal bovine serum (F7524) (Sigma) and 1% penicillin streptomycin (P0781) (Sigma) and maintained at 37 °C in a humidified 5% CO2 atmosphere. To analyse the effects of Norgestrel on 661W cells, one million cells were seeded in a T75 flask and allowed to attach overnight. Cells were then washed three times with warmed phosphate-buffered saline (PBS, pH 7.4) and complete or serum-free medium supplemented with 20 μM Norgestrel or the equivalent DMSO (1:2,500) control was added. Cells undergoing specific inhibition treatments were pre-treated for 10 minutes in serum-free media supplemented with AG205 (1 - 10 μM), dantrolene sodium salt (1 μM), calcium chelator EGTA (0.5 mM) or L-type Ca^{2+} channel blocker Verapamil (10 - 100 μM). 20 μM Norgestrel or the equivalent DMSO (1:2,500) control was then added directly to the flasks. After incubation for the indicated times, cells were washed with ice-cold PBS and detached using accutase solution (A6964) (Sigma). Cells were then spun down to leave a whole cell pellet.

Flow Cytometry: Measurement of intracellular Ca^{2+}

Cytoplasmic Ca^{2+} levels were determined using the probe Fluo-4 AM. 30 minutes prior to treatment conclusion, 1 μM Fluo-4 AM was added directly to the cells and incubated at 37 °C in the dark. After 30 minutes incubation, cells were washed with 1 x PBS, detached and spun down to form a whole cell

pellet. Cells were then resuspended in Ca^{2+} Fluo-4 AM cell loading medium: 10 % HBSS (#14180-046) (Gibco), 1 mM $CaCl_2 2H_2O$ (#223506) (Sigma), 1 mM $MgCl_2$ (M8266) (Sigma), 1 % foetal bovine serum (F7524) (Sigma), before analysis on a FACScan flow cytometer (Becton Dickinson, Oxford, UK). Intracellular Ca^{2+} production was measured at FL-1 (530 nm) with excitation at 488 nm. FACScan flow cytometer was calibrated using rainbow calibration particles (Becton Dickinson), by a certified Becton Dickinson engineer. CellQuest software (Becton Dickinson) was used for data analysis. Untreated 661W cell viability was previously confirmed using the MTS assay. Healthy cells were subsequently taken for analysis by flow cytometry and a distinct cell population was observed. This population was tightly gated (Figure 2A) and this gate was carried forward for use in all readings of subsequent treatments. Therefore only viable cells were included in Fluo-4 AM analyses. A total of 10,000 gated events per sample were acquired. All FACS analyses were carried out in technical triplicates and all graphs represent data obtained from three independent experiments.

Live Cell Imaging: Visualisation of intracellular Ca^{2+}

Cells required for visualisation of intracellular Ca^{2+} were seeded overnight (25×10^3 per plate) in 35 mm with 20 mm micro-well glass bottomed dishes (MatTek, MA, USA). Cells were then washed three times in 1 x PBS before treatment. Cytoplasmic Ca^{2+} levels were determined using the probe Fluo-4 AM. 30 minutes prior to treatment conclusion, 1 μM Fluo-4 AM was added directly to the cells and incubated at 37 °C in the dark. Cells were washed three times in warmed 1 x PBS and Ca^{2+} Fluo-4 AM cell loading medium added (see Flow Cytometry: Measurement of intracellular Ca^{2+} section). Plates were taken immediately to the confocal microscope and confocal micrographs imaged using an Olympus Fluoview FV1000 laser scanning confocal microscope, 20 x objectives. Images were taken using the software Olympus Fluoview Ver 4.1a and are represented as single slices in the XY plane. Identical microscope settings were used when visualising specific markers across all time points and treatments.

Immunofluorescence

661W cells (25×10^3 per well) were seeded overnight in 24 well plates (Starstedt) with glass coverslips. After treatment, cells were fixed with 4 % PFA for 10 minutes at room temperature. Cells were then blocked and permeabilised in 0.1 % Triton X-100 and 5 % donkey serum in 1 x PBS for 10 minutes and incubated with primary antibody diluted in 5% donkey serum overnight at 4 °C. Following washes, coverslips were incubated with conjugated secondary antibody (1:500) and Hoechst (0.1 μg/ml) for 1h at room temperature. Eliminating the primary antibody in solution served as a negative control. Coverslips were mounted on to glass slides using Mowiol.

Microscopy

Cell preparations were viewed using a Leica DM LB2 microscope with Nikon Digital Sight DS-U2 camera, using 40 x objectives. Images were taken using the software NIS-Elements version 3.0, Nikon, Japan. Immunofluorescence on cell preparations was performed in triplicate. Identical microscope settings were used when visualising markers across all treatments.

Assessment of cell viability

MTS assay was used to quantify cellular viability after serum starvation and treatment with either AG205 or EGTA. Cells seeded overnight (2 x 10^3 per well) in flat bottomed 96 well plates (Starstedt) to allow for cell adherence. These were then washed three times in 1 x PBS before treatment. After 20 h of treatment incubation, 20 µl of MTS solution was added to each well and incubated for a further 4 h at 37 °C. Viable cells in the presence of phenazine methosulfate (PMS) will reduce the MTS solution to form formazan. Detection and quantification of the formazan crystals is then carried out with a microplate reader (Molecular Device Corporation, Spectramax Plus 384, Sunnyvale, CA, USA) at 490 nm. 490 nm readings taken from non-template wells (media and MTS, without cells) were deducted from actual cellular readings. A further reading at 650 nm was also taken from all wells and deducted from the 490 nm readings to account for any cellular debris. The quantity of formazan product as measured by the amount of 490 nm absorbance, is directly proportional to the number of living cells in culture. Therefore the absorbance of the formazan formed in 'control cell wells', i.e. non-serum starved, healthy 661W cells, was taken as 100 % viability.

Total RNA Isolation and quantitative real time PCR (rt-qPCR)

Total RNA was isolated from whole cells using RNeasy Mini Kit (Qiagen, West Sussex, UK) following manufacturer's protocol. All samples were DNase treated using RNase free DNase set (Qiagen) and cDNA was synthesised using QuantiTect Reverse Transcription Kit (Qiagen) according to manufacturer's instructions. Rt-qPCR was performed on 1 µg DNA-free RNA using QuantiTect SYBR Green PCR Kit (Qiagen) on a 384 well plate (Starstedt AG & Co.). Plates were run using the Applied Biosystems 7900HT Fast Real-Time PCR System (Life Technologies Ltd., Paisley, UK) and each set of reactions included both a non-reverse transcription control and a no template sample negative control (data not shown). The protocol consisted of a cycling profile of 30 s at 95 °C, 60s at 60 °C, and 30 s at 72 °C for 40 cycles. Melt curve analysis confirmed that a single PCR product was present. Relative changes in gene expression were quantified using the comparative Ct (ΔΔCt) method as described by Livak & Schmittgen (2001; Schmittgen & Livak, 2008). The Ct value of the gene of interest was normalised to an average of the three endogenous housekeeping genes (Actb, Gapdh, Hprt). This was then compared to the normalised control sample – the equivalent DMSO (1:2,500) timed control. Alteration in mRNA expression of target genes was defined as fold difference in the expression level in cells after treatment, relative to that of the control.

siRNA Transfection

Cells were seeded overnight prior to transfection in T75 flasks (300 x 10^3) (Starstedt) to allow for cell adherence. Transfected cells (25 nM FGF2 siRNA and 25 nM Allstars Negative Control siRNA) were left for 48 h before treatment. Cells were washed three times in warmed phosphate-buffered saline (PBS, pH 7.4) before serum-free medium supplemented with 20 µM Norgestrel or the equivalent DMSO (1:2,500) control was added.

Statistical analyses

All data was tested for normality D'Agostino-Pearson omnibus test before subsequent statistical analysis by Student t-test or one-way ANOVA. ANOVAs were followed by either a Dunnett's or Tukey's multiple comparisons test, depending upon whether all data points were being compared to each test group, or to the untreated control (Graph Pad, Prism 6). Values of $p < 0.05$ were considered statistically significant.

Results

Norgestrel induces an increase in intracellular Ca^{2+} levels in healthy 661W photoreceptor-like cells over 3 hours

Changes in $[Ca^{2+}]_i$ mediate many critical signalling processes in neurons (Berridge 1997; Koulen and Thrower 2001). Knowing this, we wished to determine if changes in $[Ca^{2+}]_i$ occurred in photoreceptors in response to the neuroprotective synthetic progestin Norgestrel (Doonan *et al.*, 2011; Wyse-Jackson & Cotter, 2016; Wyse-Jackson *et al.*, 2016). Healthy 661W photoreceptor-like cells were treated with 20μM Norgestrel (Norgestrel) or equivalent DMSO control (DMSO) over 3 and 24 hours. A healthy cell population was gated (Figure 2A) and an increase in intracellular calcium was detected using the specific intracellular calcium probe Fluo-4 AM. Norgestrel significantly increased $[Ca^{2+}]_i$ levels in 661W cells over 3 hours but these changes were back down to control levels after 24 hours (Figure 2Bi, ii). All timed treatments are graphed compared to untreated control (Figure 2Bii; unpaired t-test comparing Norgestrel treatments to timed DMSO control, two-tailed, $df = 16$, 3 h $P = 1.247 \times 10^{-7}$, 24 h $P = 0.06987$).

Serum withdrawal induces an increase in intracellular Ca^{2+} levels in 661W photoreceptor-like cells

Previous studies from our group have shown that the protective effects of Norgestrel on photoreceptor cells, is dependent upon cellular stress (Wyse-Jackson & Cotter, 2016). Knowing this, we have consistently showed that deprivation of trophic factor support will induce cell death in 661W cells and have subsequently found it to be a suitable *in vitro* model by which to study photoreceptor cells in the diseased state (Gómez-Vicente *et al.*, 2005; Byrne *et al.*, 2016; Wyse-Jackson & Cotter, 2016; Wyse-Jackson *et al.*, 2016). Therefore, we serum starved 661W cells and measured the resulting changes in $[Ca^{2+}]_i$. Serum starvation alone significantly increased $[Ca^{2+}]_i$ in 661W cells three-fold over one hour compared to untreated control (Figure 3A, C). This increase was maintained over three hours, but returned to normal, untreated levels after 24 hours of serum deprivation. All treatments are graphed compared to untreated control (Figure 3Aii; one-way ANOVA followed by Dunnett's multiple comparisons test comparing timed serum starvation to untreated control. $F_{5,87} = 34.01$, $P < 0.0001$).

Live imaging of 661W cells show the extent to which serum starvation affects cellular morphology. Short periods (30 mins, 1 h) of serum starvation causes an initial retraction of cellular processes, likely as a stress response. Cells begin to settle again however after about 2 to 3 hours, extending their processes out once again (Figure 3B). MTS viability assay of serum starved cells confirmed this result

with cells stressed for 30 minutes and 1 hour showing significant decreases in cell viability compared to healthy untreated control cells. Cell viability has returned to normal levels after 3 hours (Figure 3D). The MTS assay assesses cellular viability as a measure of formazan production, comparing healthy, untreated cells to treated cells. Therefore, changes in proliferation or metabolism by these cells will decrease the amount of formazan produced: these cells will be classed as less 'viable' than the 100 % viable control. This is likely the case 30 minutes and 1 hour after serum starvation (Figure 3D). The stressor decreases cellular metabolism of the MTS solution, producing less formazan and thus the cells are significantly less 'viable' that the 100 % viable untreated control. Once the cells settle again (2 to 3 hours; Figure 3B), viability is returned to normal levels (Figure 3D). Live imaging of intracellular calcium in serum starved 661W cells corroborates this morphological change and supports the FACs quantification of intracellular calcium increases following serum starvation (Figure 3C).

Norgestrel sustains an increase in intracellular Ca^{2+} levels over 24 hours

Progesterone signalling has been demonstrated to induce increases in cytosolic calcium (Samadi *et al.* 2002; Koulen *et al.* 2008). Therefore, further to the finding that serum deprivation drives an increase in $[Ca^{2+}]_i$; we sought to determine if administration of Norgestrel affected this signalling. 661W cells were serum starved and treated with 20 μM Norgestrel or the equivalent DMSO control for the indicated time periods. Norgestrel significantly induced a further increase in $[Ca^{2+}]_i$ over 24 hours compared to timed DMSO control (Figure 4). All treatment are graphed compared to untreated control (Figure 4C; unpaired t-test comparing Norgestrel treatments to timed DMSO control, two-tailed, df = 16, 30 mins $P = 1.948 \times 10^{-5}$, 1 h $P = 6.490 \times 10^{-11}$, 2 h $P = 5.807 \times 10^{-9}$, 3 h $P = 1.303 \times 10^{-11}$, 24 h $P = 0.0149$).

Inhibition of progesterone receptor membrane complex 1 signalling abrogates Norgestrel-induced increases in intracellular Ca^{2+}

While many progesterone receptors are present in the retina, Norgestrel has been shown to signal predominantly through progesterone receptor membrane complex one (PGRMC1) (Wyse-Jackson *et al.*, 2016). **Indeed, specific knock down or abrogation of PGRMC1 signalling will prevent the protective actions of Norgestrel both *in vitro* and *ex vivo* (Wyse-Jackson & Cotter, 2016; Wyse-Jackson *et al.*, 2016).** Therefore, we hypothesised that the increase in $[Ca^{2+}]_i$ in Norgestrel-treated stressed 661W cells was due to signalling downstream of Norgestrel-PGRMC1 binding. **siRNA abrogation of PGRMC1 has a significant detrimental effect on 661W cellular viability (Wyse-Jackson *et al.*, 2016) and thus PGRMC1 specific inhibitor AG205 was instead employed to block the effects of PGRMC1 in 661W cells.** AG205 is a potent and specific inhibitor of PGRMC1 activity. Altering the spectroscopic properties of the PGRMC1–heme complex, it has also been shown to inhibit cell cycle progression (Ahmed *et al.*, 2010), likely affecting $[Ca^{2+}]_i$. Consequently, we trialled a number of different concentrations (1 μM – 10 μM) in serum starved 661W cells to ensure $[Ca^{2+}]_i$ was not affected by the dose of AG205 used. These concentrations have been previously shown not to affect 661W cell viability (Wyse-Jackson *et al.*, 2016). Analysis by flow cytometry showed that addition of 1 μM AG205 to stressed 661W cells showed comparable levels of $[Ca^{2+}]_i$ compared to serum starved DMSO control (Figure 5A). This dose was also still able to effectively attenuate the protective effects of Norgestrel on stressed 661W cells, as measured by the MTS cell viability assay (Figure 5B; one-way ANOVA followed by Tukey's multiple comparisons test. $F_{3,99}$ = 26.64, $P < 0.0001$). Thus the 1 μM dose was taken forward to determine whether PGRMC1 was

responsible for Norgestrel-induced increases in $[Ca^{2+}]_i$ in stressed 661W cells. Serum starved 661W cells were cultured in the absence and presence of 1 μM AG205. After 10 minutes, 20 μM Norgestrel or equivalent DMSO control was added directly to the flasks and incubated for the times indicated. Stressed cells pre-treated with 1 μM AG205 do not exhibit any significant increase in $[Ca^{2+}]_i$ in response to 20 μM Norgestrel over any time point up to three hours (Figure 5Ci, ii; two-way ANOVA followed by Dunnett's multiple comparison's test comparing all treatments to timed serum starved DMSO control. $F_{12,329} = 33.41$, $P < 0.0001$). All treatments are graphed compared to untreated control (Figure 5A, Cii).

Norgestrel signals through PGRMC1 to induce an upregulation of basic fibroblast growth factor

Previous studies from this group identified bFGF signalling with sequential downstream targets of protein kinase A and glycogen synthase kinase 3β, as the major pro-survival pathway responsible for Norgestrel's neuroprotective efficacy in stressed photoreceptor cells (Doonan *et al.* 2011; Wyse Jackson and Cotter 2016). Since Norgestrel signals primarily through PGRMC1 (Wyse-Jackson *et al.*, 2016), we sought to determine if Norgestrel-PGRMC1 signalling was responsible for Norgestrel-induced increases in bFGF. 661W cells were serum starved and cultured in the absence and presence of 1 μM PGRMC1 inhibitor AG205 for 10 minutes. After this pre-treatment, 20 μM Norgestrel or equivalent DMSO control was added and cells were incubated for a further hour. Analysis by rt-qPCR showed that the Norgestrel-induced increase in bFGF mRNA in serum starved 661W cells, is abrogated by pre-treatment with AG205 (Figure 6A; one-way ANOVA followed by Tukey's multiple comparison's test. $F_{3,36} = 5.041$, $P = 0.0037$). From this, we suggest that Norgestrel-PGRMC1 signalling is responsible for the protective upregulation of bFGF.

Norgestrel-induced increases in basic fibroblast growth factor drive subsequent increases in intracellular calcium

bFGF signalling has previously been shown to directly modulate calcium activity in the retina (Lom *et al.* 1998; Niu *et al.* 2004). To investigate the potential role that bFGF plays in Norgestrel-induced changes in $[Ca^{2+}]_i$, 661W cells were treated with siRNA against bFGF over 48 hours. A significant decrease in bFGF expression (~75%) was verified through rt-qPCR (Figure 6Bi; unpaired t-test, two-tailed, $df = 6$, $P = 0.0009$) and complete protein knock down was shown by immunofluorescence (Figure 6Bii). siRNA-treated stressed cells were then treated with either DMSO of 20 μM Norgestrel for one hour and changes in $[Ca^{2+}]_i$ analysed using Fluo-4 AM. Stressed cells treated with siRNA against bFGF did not demonstrate the same Norgestrel-induced increase in $[Ca^{2+}]_i$ seen in the non-targeting scrambled control (Figure 6Ci, ii). All treatment are graphed compared to untreated control (Figure 6Cii; unpaired t-test comparing Norgestrel treatments to equivalent serum starved scrambled or siRNA DMSO control, two-tailed, $df = 22$, Scrambled $P = 5.2122 \times 10^{-17}$, bFGF $P = 0.745$).

Norgestrel induces an increase in intracellular calcium, predominantly from extracellular sources

Progesterone evokes calcium signalling in retinal cells through both an activation of intracellular stores (Sharma & Rohrer, 2004) and through entry of extracellular calcium into the cell (Samadi *et al.*, 2002; Swiatek-De Lange *et al.*, 2007). However, the source of increased $[Ca^{2+}]_i$ in stressed 661W cells in response to Norgestrel is unknown. To evaluate this, the effect of both of IP3/ryanodine

receptor antagonists (dantrolene) and an extracellular calcium chelator (EGTA) (Healy *et al.*, 2013) on Norgestrel-induced $[Ca^{2+}]_i$ elevations were examined. Dantrolene sodium salt inhibits the release of Ca^{2+} from sarcoplasmic reticulum stores by antagonising ryanodine receptor (RYR) channels, decreasing the amount of available intracellular calcium. Displaying selectivity for RYR1 and RYR3 over RYR2, dantrolene is often used as a muscle relaxant, decreasing excitation-contraction coupling in muscle cells (Zucchi & Ronca-Testoni, 1997). EGTA is an aminopolycarboxylic acid chelating agent that cannot pass through the cell membrane, due to its size. Related to EDTA, it has a lower affinity for magnesium, making it more selective for calcium ions in free solution.

661W cells were serum starved and pre-treated for ten minutes with 0.5 mM EGTA or 1 μM dantrolene. After this incubation period, cells were directly stimulated with 20 μM Norgestrel or equivalent DMSO control. Cells pre-treated with 0.5 mM EGTA did not show complete abrogation of Norgestrel-induced $[Ca^{2+}]_i$ increase. Indeed, Norgestrel still managed to increase intracellular calcium levels by about 2-fold compared to EGTA pre-treated control (Figure 7Aii). However, the Norgestrel-induced increase in $[Ca^{2+}]_i$ following EGTA treatment was only comparable to the levels of serum starved control (Figure 7Ai, ii) – and $[Ca^{2+}]_i$ was not driven up beyond this level. Alternately, cells pre-treated with 1 μM dantrolene did not show any difference in Norgestrel induced $[Ca^{2+}]_i$ compared to non-pre-treated serum starved Norgestrel control. Despite dantrolene pre-treatment, Norgestrel was still able to drive $[Ca^{2+}]_i$ to a response equal to that of Norgestrel without dantrolene pre-treatment. All taken, this indicates that the rise in $[Ca^{2+}]_i$ in stressed 661W cells in response to Norgestrel is not due to cytosolic influx from intracellular stores. A double control whereby both extracellular calcium was chelated and intracellular IP3/ryanodine receptors were antagonised was carried out to account for possible compensation between these sources. Stressed cells pre-treated with both 0.5 mM EGTA and 1 μM dantrolene showed only a slight, non-significant increase in $[Ca^{2+}]_i$, compared to control (Figure 7Ai, ii). Taken together, these data suggest that Norgestrel-evoked calcium signalling utilises calcium predominantly from an extracellular source. However, Norgestrel-evoked increases in $[Ca^{2+}]_i$ following EGTA pre-treatment infer that there is some degree of compensation occurring from intracellular sources, when the preferred extracellular sources are blocked (Figure 7Aii; unpaired t-test comparing Norgestrel treatments to specific pre-treated DMSO control, two-tailed, $df = 16$, DMSO $P = 7.08 \times 10^{-7}$, EGTA $P = 1.5424 \times 10^{-6}$, Dantrolene $P = 0.0003$, EGTA + Dantrolene $P = 0.0827$).

To further verify that the raised $[Ca^{2+}]_i$ following Norgestrel treatment is indeed coming from extracellular sources, we pre-treated cells with L-type Ca^{2+} channel blocker verapamil (Liu *et al.*, 2016), to prevent influx through these channels. We tested a number of concentrations (10 – 100 μM) so as to investigate the effect of verapamil on $[Ca^{2+}]_i$ in untreated cells. Unfortunately, all concentrations caused $[Ca^{2+}]_i$ in untreated cells to rise. However, since 10 μM and 50 μM induced the same $[Ca^{2+}]_i$ increase (Figure 7Bi; one-way ANOVA followed by Dunnett's multiple comparisons test. $F_{3,8} = 35.34$, $P < 0.0001$), and since previous ocular research has found 50 μM verapamil to successfully block calcium passage through L-type calcium channels (Liu *et al.*, 2016); we carried this concentration forward to look at the role of L-type calcium channels in Norgestrel-induced extracellular calcium influx. 661W cells were serum starved and pre-treated for ten minutes with 50 μM verapamil. After this incubation period, cells were directly stimulated with 20 μM Norgestrel or equivalent DMSO control. Cells pre-treated with 50 μM did not see the same Norgestrel-induced rise in $[Ca^{2+}]_i$ compared to the non-verapamil treated serum starved cells (Figure 7Bii; unpaired t-test comparing Norgestrel treatments to specific pre-treated DMSO control, two-tailed, $df = 16$, Serum

Starved $P = 0.00072$, Serum Starved + Verapamil $P = 0.9415$). Although verapamil treatment alone induced a large increase in $[Ca^{2+}]_i$, this rise is comparable to the rise in $[Ca^{2+}]_i$ seen in the verapamil dose response in Figure 7Bi. Importantly, there was no change in verapamil pre-treated cells administered with DMSO or Norgestrel (Figure 7Bii). All taken, these data suggest that the Norgestrel-induced rise in $[Ca^{2+}]_i$ is predominantly from extracellular sources, influxing through L-type calcium channels.

The protection afforded to Norgestrel-treated stressed 661W cells is abrogated through specific extracellular calcium chelation by EGTA

Norgestrel significantly inhibits 661W cells from serum starved cell death over 24 hours, as measured by the MTS cell viability assay (Figure 5B). Having established that administration of Norgestrel causes an upregulation of $[Ca^{2+}]_i$ over 24 hours (Figure 4) and that this increase is coming predominantly from extracellular sources (Figure 7A, B), we then sought to determine whether $[Ca^{2+}]_i$ is required for the neuroprotective effects afforded by Norgestrel. Serum starved 661W cells were cultured with EGTA (0.5 mM) and simultaneously treated with either DMSO or 20 μM Norgestrel over 24 hours. No change in viability of these cells was determined compared to the relevant serum starved DMSO control (Figure 7C; one-way ANOVA followed by Tukey's multiple comparisons test. $F_{5,137} = 18.09$, $P < 0.0001$), thus extracellular calcium chelation by EGTA abrogated Norgestrel's neuroprotective effects on stressed 661W cells.

Discussion

In this study, we further elucidate the pathway leading to photoreceptor neuroprotection by the synthetic progesterone analogue 'Norgestrel'. **Experimentally outlined in Figure 1B**, we show by flow cytometry, live-cell immunofluorescence, real-time PCR and cell viability assays that Norgestrel, acting through PGRMC1, induces an upregulation of bFGF – previously found to be critical in mediating Norgestrel's neuroprotective effects. The upregulation of bFGF subsequently induces an influx of calcium in to the cell, primarily from extracellular sources. Finally, we hypothesise that this increase in intracellular calcium is essential in Norgestrel-mediated neuroprotection, for blockade of this influx prevents the actions of Norgestrel on stressed 661W photoreceptor cells **(Figure 1A).**

Norgestrel significantly increases intracellular calcium in photoreceptor-like cells following trophic factor deprivation

Whilst some cellular signals are regulated by rapid and transient calcium increases, others are designed to produce longer-lasting global elevations of calcium (Berridge and Dupont 1994; Lopez *et al.* 2012). These sustained increases in intracellular calcium following neurological insult are often stated to be responsible for neuronal cell death (Frasson *et al.* 1999; Sharma and Rohrer 2004; Rodríguez-Muela *et al.* 2014). Unfortunately, this is an oversimplification, for the susceptibility of cells to calcium-induced neurotoxicity depends on a number of different factors (Friedman, 2006).

For example, the time span of calcium signalling vs. the concentration of intracellular cytosolic calcium is known to vary the anti- vs. pro-apoptotic capabilities of calcium signalling (Berridge *et al.*, 2003). Indeed, evidence is now also mounting to suggest a neuroprotective role of calcium in activating downstream pro-survival signalling (Bickler and Fahlman 2004; Swiatek-De Lange *et al.* 2007) and in regulation of cell cycle, proliferation, apoptosis, gene transcription, and cell migration (Berridge *et al.*, 2003; Déliot & Constantin, 2015).

Progesterone signalling has previously been shown to affect retinal cytosolic calcium concentrations, though with such a variety of potential signalling capabilities, the role this plays in retinal neuroprotection is still unclear (Samadi *et al.* 2002; Luoma *et al.* 2012; Koulen *et al.* 2008). Nevertheless, studies exist highlighting potential protective roles of progesterone-induced retinal calcium signalling. **For example, in 2010, Andreas Bringmann's group in the Universität Leipzig showed that progesterone activated voltage gated calcium channels, causing $[Ca^{2+}]_i$ levels to rise. Activating the glutamatergic-purinergic signalling cascade, this consequently inhibits retinal glial cell swelling, preventing cytotoxic retinal oedema (Neumann *et al.*, 2010). Retinal progesterone-induced calcium signalling is further corroborated in the retina in a study showing that progesterone-PGRMC1 binding induces calcium influx in to Müller glial cells (Swiatek-De Lange *et al.*, 2007). In this study, we consistently show that Norgestrel induces a large influx in $[Ca^{2+}]_i$ in stressed 661W cells. Moreover, we show that this influx is necessary for the induction of Norgestrel's neuroprotective actions (Figure 7C), further strengthening the claim that in this model of retinal degeneration, calcium signalling is protective.**

Norgestrel-PGRMC1 binding induces an increase in neuroprotective bFGF, which drives a subsequent rise in intracellular calcium

In separate works from this laboratory, the actions of Norgestrel have been shown to act critically, through both PGRMC1 activation and bFGF upregulation (Wyse-Jackson & Cotter, 2016; Wyse-Jackson *et al.*, 2016). In this study, we show through pre-treatment with PGRMC1-specific inhibitor AG205, that Norgestrel-PGRMC1 binding is responsible for the Norgestrel-induced increase in $[Ca^{2+}]_i$ in stressed 661W cells (Figure 5Ci, ii). However, the link to neuroprotective bFGF has not yet been elucidated. Previous research shows the potential of bFGF to modulate calcium channels, consequently affecting $[Ca^{2+}]_i$ (Puro and Mano 1991; Rosenthal *et al.* 2005; Zamburlin *et al.* 2013). Thus we proposed the following pathway of Norgestrel-induced neuroprotection: Norgestrel activates PGRMC1 expressed on the surface of photoreceptor cells. This activation will drive the upregulation of bFGF which will subsequently affect $[Ca^{2+}]_i$ (Figure 1).

In order to verify this hypothesis, stressed 661W cells treated with Norgestrel and/or PGRMC1 inhibitor AG205, were examined for bFGF upregulation. As in previous work, bFGF mRNA was upregulated in stressed 661W cells after one hour in response to Norgestrel (Figure 6A) – a process critical to Norgestrel-induced cellular protection (Wyse-Jackson & Cotter, 2016). However, cells pre-treated with AG205 did not exhibit this same increase in bFGF mRNA (Figure 6A). Therefore, we conclude that activation of PGRMC1 is necessary for the Norgestrel-induced upregulation of neuroprotective bFGF (Désiré *et al.* 2000; O'Driscoll *et al.* 2007; O'Driscoll *et al.* 2008; Yang *et al.*

2014). Moreover, we found that when the actions of bFGF are attenuated by siRNA (Figure 6B), Norgestrel can no longer stimulate an increase in $[Ca^{2+}]_i$ (Figure 6Ci, ii). These data suggest that Norgestrel-PGRMC1 binding leads to bFGF upregulation with a successive influx of neuroprotective cytosolic calcium (Figure 7C).

Norgestrel-mediated increases in intracellular calcium come predominantly from extracellular sources

Cellular calcium levels can be raised through calcium release from both intracellular stores and extracellular sources. These sources differ in their release mechanisms. Extracellular calcium influxes through activation of plasma membrane calcium channels. These include both voltage-gated and non-voltage gated channels, though calcium entry in excitable cells such as photoreceptors occurs mostly though voltage-gated channels (Berridge *et al.* 2003; Déliot and Constantin 2015). Alternately, intracellular calcium is released into the cytosol through ligand gated receptor-operated calcium channels, the most recognised being the inositol triphosphate (IP_3) and ryanodine receptors found on the endoplasmic and sarcoplasmic reticulum (Bennett *et al.* 1996; Wójcik-piotrowicz *et al.* 2016). Release of calcium from either extra- or intracellular stores will lead to differential activation of cellular mechanisms, for many cellular activities are preferentially activated by different $[Ca^{2+}]_i$ (Berridge *et al.* 2003; Wójcik-piotrowicz *et al.* 2016). For example, internal stores hold a large but finite amount of calcium and thus will activate processes that do not require sustained influxes of calcium that are more typical of extracellular sources (Berridge and Dupont 1994; Bootman and Berridge 1995; Berridge 1997). For this reason, the source of calcium released in stressed 661W cells in response to Norgestrel administration was of interest.

Using the IP3/ryanodine receptor antagonist dantrolene and extracellular calcium chelator EGTA (Healy *et al.*, 2013), we found that the source of calcium released in stressed 661W cells in response to Norgestrel administration was primarily from extracellular sources (Figure 7Ai, ii). **Certainly however, there appears to be some compensation from intracellular stores when extracellular sources are blocked: Norgestrel could not stimulate as large an increase in $[Ca^{2+}]_i$ when dantrolene and EGTA were used in combination, as when EGTA was used alone (Figure 7Aii).**

Since Norgestrel induced rises in $[Ca^{2+}]_i$ appear to come predominantly from extracellular sources, we next looked to see if this influx occurs through voltage-gated calcium channels (Berridge *et al.* 2003; Déliot and Constantin 2015). These channels have previously been shown to be activated in response to progesterone (Neumann *et al.*, 2010). Pre-treatment with L-type Ca^{2+} channel blocker verapamil successfully prevented a Norgestrel-induced rise in $[Ca^{2+}]_i$ in stressed 661W cells as compared to verapamil pre-treated DMSO control (Figure 7Bii). Finally, we aimed to determine extracellular calcium was necessary for Norgestrel-induced neuroprotection of stressed 661W cells. Serum starved cells pre-treated with a concentration of EGTA that does not affect cell viability (0.5 M, Figure 7C), did not display an increase in cell viability when treated with Norgestrel. All taken, we hypothesise that a Norgestrel-induced rise in $[Ca^{2+}]_i$, occurring primarily through extracellular calcium influx through voltage gated calcium channels (Figure 7Bii), is required for Norgestrel's pro-survival activities (Figure 7C).

Norgestrel-signalling potentially acts through calcium-dependent activation of adenylate cyclase

Calcium is becoming more prevalent in the literature as a pro-survival signalling molecule, affecting both cellular proliferative and apoptotic processes (Berridge *et al.* 2003; Bickler and Fahlman 2004; Swiatek-De Lange *et al.* 2007; Déliot and Constantin 2015). One potential mechanism by which calcium signalling may be neuroprotective in this system is by the calcium-dependent activation of adenylate cyclase (AC). AC, once activated, can produce cAMP to mediate PKA activation (Sancho-Pelluz *et al.*, 2008), previously shown by our laboratory to be critical in the neuroprotective actions of Norgestrel on stressed photoreceptor cells (Wyse-Jackson & Cotter, 2016). Active PKA can then phosphorylate and activate cAMP response element binding protein (CREB), a transcription factor crucial for neuronal survival (Finkbeiner 2000; Mantamadiotis *et al.* 2002). Since bFGF, driven up by Norgestrel (Figure 6A) (Doonan *et al.*, 2011; Wyse-Jackson & Cotter, 2016), can promote the phosphorylation of CREB via PKA (O'Driscoll *et al.*, 2007), we hypothesise that Norgestrel signals through the calcium dependent, cAMP-AC-PKA pathway to protect stressed photoreceptors. Further research will have to be carried out to substantiate this claim however.

In this study, we have further elucidated the potential of Norgestrel to upregulate pro-survival signalling activities in stressed photoreceptor cells through PGRMC1 receptor binding**. A schematic overview of the results of this study is presented in Figure 1.** We reveal a novel role for PGRMC1 activation in the upregulation of bFGF, a growth factor shown previously to be crucial to Norgestrel's neuroprotective capabilities. In addition to this, we show through specific siRNA knock down, that bFGF is responsible for the Norgestrel-induced increase in cytosolic calcium, in stressed 661W cells. Hypothesised to influx primarily from extracellular stores through voltage-gated calcium channels, we believe this increase in cytosolic calcium to be essential in regulating Norgestrel's pro-survival capacity, for calcium chelation by EGTA abrogates the protective properties of Norgestrel on stressed 661W cells *in vitro*.

Conflict of interest

The authors declare no competing interests.

Acknowledgements

This work was supported by Fighting Blindness Ireland and Science Foundation Ireland.

Abbreviations

AC: Adenylate cyclase

AKT: Protein Kinase B

bFGF: Basic fibroblast growth factor

$[Ca^{2+}]_i$: Intracellular calcium concentration

CREB: cAMP response element-binding protein

MAPK: Mitogen-activated protein kinases

PGRMC1: Progesterone receptor membrane component 1

PKA: Protein kinase A

PKC: Protein kinase C

RP: Retinitis pigmentosa

Rt-qPCR: Real time quantitative polymerase chain reaction

siRNA: Small interfering ribonucleic acid

TUNEL: Terminal dUTP Nick-End Labelling

Bibliography

Ahmed, I.S., Rohe, H.J., Twist, K.E., Mattingly, M.N., & Craven, R.J. (2010) Progesterone receptor membrane component 1 (Pgrmc1): a heme-1 domain protein that promotes tumorigenesis and is inhibited by a small molecule. *J. Pharmacol. Exp. Ther.*, **333**, 564–573.

Ait-Hmyed, O., Felder-Schmittbuhl, M.-P., Garcia-Garrido, M., Beck, S., Seide, C., Sothilingam, V., Tanimoto, N., Seeliger, M., Bennis, M., & Hicks, D. (2013) Mice lacking Period 1 and Period 2 circadian clock genes exhibit blue cone photoreceptor defects. *Eur. J. Neurosci.*, **37**, 1048–1060.

Allen, R.S., Olsen, T.W., Sayeed, I., Cale, H.A., Morrison, K.C., Oumarbaeva, Y., Lucaciu, I., Boatright, J.H., Pardue, M.T., & Stein, D.G. (2015) Progesterone treatment in two rat models of ocular ischemia. *Invest. Ophthalmol. Vis. Sci.*, **56**, 2880–2891.

Bennett, D.L., Cheek, T.R., Berridge, M.J., De Smedt, H., Parys, J.B., Missiaen, L., & Bootman, M.D. (1996) Expression and function of ryanodine receptors in nonexcitable cells. *J. Biol. Chem.*, **271**, 6356–6362.

Berridge, M.J. & Dupont, G. (1994) Spatial and temporal signalling by calcium. *Curr. Opin. Cell Biol.*, **6**, 267–274.

Berridge, M.J. (1997) Annual Review Prize Lecture: Elementary and global aspects of calcium signalling. *J. Physiol.*, **499**, 291–306.

Berridge, M.J., Bootman, M.D., & Roderick, H.L. (2003) Calcium signalling: dynamics, homeostasis and remodelling. *Nat. Rev. Mol. Cell Biol.*, **4**, 517–529.

Bickler, P.E. & Fahlman, C.S. (2004) Moderate increases in intracellular calcium activate neuroprotective signals in hippocampal neurons. *Neuroscience*, **127**, 673–683.

Bootman, M.D. & Berridge, M.J. (1995) The elemental principles of calcium signaling. *Cell*, **83**, 675–678.

Byrne, A.M., Roche, S.L., Ruiz-Lopez, A.M., Wyse-Jackson, A.C., & Cotter, T.G. (2016) The synthetic progestin norgestrel acts to increase LIF levels in the rd10 mouse model of retinitis pigmentosa. *Mol. Vis.*, **22**, 264–274.

Compagnone, N.A. (2008) Treatments for spinal cord injury: is there hope in neurosteroids? *J. Steroid Biochem. Mol. Biol.*, **109**, 307–313.

Daiger, S.P., Sullivan, L.S., & Bowne, S.J. (2013) Genes and mutations causing retinitis pigmentosa. *Clin. Genet.*, **84**, 132–141.

Déliot, N. & Constantin, B. (2015) Plasma membrane calcium channels in cancer: Alterations and consequences for cell proliferation and migration. *Biochim. Biophys. Acta*, **1848**, 2512–2522.

Désiré, L., Courtois, Y., & Jeanny, J.C. (2000) Endogenous and exogenous fibroblast growth factor 2 support survival of chick retinal neurons by control of neuronal neuronal bcl-x(L) and bcl-2 expression through a fibroblast growth factor receptor 1- and ERK-dependent pathway. *J. Neurochem.*, **75**, 151–163.

Doonan, F., O'Driscoll, C., Kenna, P., & Cotter, T.G. (2011) Enhancing survival of photoreceptor cells in vivo using the synthetic progestin Norgestrel. *J. Neurochem.*, **118**, 915–927.

Doonan, F. & Cotter, T.G. (2012) Norgestrel may be a potential therapy for retinal degenerations. *Expert Opin. Investig. Drugs*, **21**, 579–581.

Espinosa-García, C., Aguilar-Hernández, A., Cervantes, M., & Moralí, G. (2014) Effects of progesterone on neurite growth inhibitors in the hippocampus following global cerebral ischemia. *Brain Res.*, **1545**, 23–34.

Finkbeiner, S. (2000) CREB couples neurotrophin signals to survival messages. *Neuron*, **25**, 11–14.

Frasson, M., Sahel, J.A., Fabre, M., Simonutti, M., Dreyfus, H., & Picaud, S. (1999) Retinitis pigmentosa: rod photoreceptor rescue by a calcium-channel blocker in the rd mouse. *Nat. Med.*, **5**, 1183–1187.

Friedman, L.K. (2006) Calcium: A role for neuroprotection and sustained adaptation. *Mol. Interv.*, **6**, 315–329.

Garay, L., Tüngler, V., Deniselle, M.C.G., Lima, A., Roig, P., & De Nicola, A.F. (2011) Progesterone attenuates demyelination and microglial reaction in the lysolecithin-injured spinal cord. *Neuroscience*, **192**, 588–597.

Gómez-Vicente, V., Donovan, M., & Cotter, T.G. (2005) Multiple death pathways in retina-derived 661W cells following growth factor deprivation: crosstalk between caspases and calpains. *Cell Death Differ.*, **12**, 796–804.

Gonzalez Deniselle, M.C., Lopez Costa, J.J., Gonzalez, S.L., Labombarda, F., Garay, L., Guennoun, R., Schumacher, M., & De Nicola, A.F. (2002a) Basis of progesterone protection in spinal cord neurodegeneration. *J. Steroid Biochem. Mol. Biol.*, **83**, 199–209.

Gonzalez Deniselle, M.C., López-Costa, J.J., Saavedra, J.P., Pietranera, L., Gonzalez, S.L., Garay, L., Guennoun, R., Schumacher, M., & De Nicola, A.F. (2002b) Progesterone neuroprotection in the Wobbler mouse, a genetic model of spinal cord motor neuron disease. *Neurobiol. Dis.*, **11**, 457–468.

Gonzalez, S.L., Labombarda, F., Gonzalez Deniselle, M.C., Mougel, A., Guennoun, R., Schumacher, M., & De Nicola, A.F. (2005) Progesterone neuroprotection in spinal cord trauma involves up-regulation of brain-derived neurotrophic factor in motoneurons. *J. Steroid Biochem. Mol. Biol.*, **94**, 143–149.

Guerin, M.B., Donovan, M., McKernan, D.P., O'Brien, C.J., & Cotter, T.G. (2011) Age-dependent rat retinal ganglion cell susceptibility to apoptotic stimuli: implications for glaucoma. *Clin. Experiment. Ophthalmol.*, **39**, 243–251.

Healy, L.M., Sheridan, G.K., Pritchard, A.J., Rutkowska, A., Mullershausen, F., & Dev, K.K. (2013) Pathway specific modulation of S1P1 receptor signalling in rat and human astrocytes. *Br. J. Pharmacol.*, **169**, 1114–1129.

Koch, S., Sothilingam, V., Garcia Garrido, M., Tanimoto, N., Becirovic, E., Koch, F., Seide, C., Beck, S.C., Seeliger, M.W., Biel, M., Mühlfriedel, R., & Michalakis, S. (2012) Gene therapy restores vision and delays degeneration in the CNGB1(-/-) mouse model of retinitis pigmentosa. *Hum. Mol. Genet.*, **21**, 4486–4496.

Koulen, P. & Thrower, E.C. (2001) Pharmacological modulation of intracellular Ca(2+) channels at the single-channel level. *Mol. Neurobiol.*, **24**, 65–86.

Koulen, P., Madry, C., Duncan, R.S., Hwang, J., Nixon, E., Mcclung, N., Gregg, E. V, & Worth, F. (2008) Progesterone Potentiates IP(3)-Mediated Calcium Signaling Through Akt/PKB. *Cell. Physiol. Biochem.*, **21**, 161–172.

Liu, X., Grove, J.C.R., Hirano, A.A., Brecha, N.C., & Barnes, S. (2016) Dopamine D1 receptor modulation of calcium channel currents in horizontal cells of mouse retina. *J. Neurophysiol.*, **116**, 686–697.

Livak, K.J. & Schmittgen, T.D. (2001) Analysis of relative gene expression data using real-time quantitative PCR and the 2(-Delta Delta C(T)) Method. *Methods*, **25**, 402–408.

Lom, B., Höpker, V., McFarlane, S., Bixby, J.L., & Holt, C.E. (1998) Fibroblast growth factor receptor signaling in Xenopus retinal axon extension. *J. Neurobiol.*, **37**, 633–641.

Lopez, L., Piegari, E., Sigaut, L., & Ponce Dawson, S. (2012) Intracellular calcium signals display an avalanche-like behavior over multiple lengthscales. *Front. Physiol.*, **3**, 350.

Lu, N., Li, C., Cheng, Y., & Du, A.-L. (2008) Protective effects of progesterone against high

intraocular pressure-induced retinal ischemia-reperfusion in rats. *J. South. Med. Univ.*, **28**, 2026–2029.

Luoma, J.I., Stern, C.M., & Mermelstein, P.G. (2012) Progesterone inhibition of neuronal calcium signaling underlies aspects of progesterone-mediated neuroprotection. *J. Steroid Biochem. Mol. Biol.*, **131**, 30–36.

Mantamadiotis, T., Lemberger, T., Bleckmann, S.C., Kern, H., Kretz, O., Martin Villalba, A., Tronche, F., Kellendonk, C., Gau, D., Kapfhammer, J., Otto, C., Schmid, W., & Schütz, G. (2002) Disruption of CREB function in brain leads to neurodegeneration. *Nat. Genet.*, **31**, 47–54.

Mookherjee, S., Hiriyanna, S., Kaneshiro, K., Li, L., Li, Y., Li, W., Qian, H., Li, T., Khanna, H., Colosi, P., Swaroop, A., & Wu, Z. (2015) Long-term rescue of cone photoreceptor degeneration in retinitis pigmentosa 2 (RP2)-knockout mice by gene replacement therapy. *Hum. Mol. Genet.*, **24**, 6446–6458.

Neumann, F., Wurm, A., Linnertz, R., Pannicke, T., Iandiev, I., Wiedemann, P., Reichenbach, A., & Bringmann, A. (2010) Sex steroids inhibit osmotic swelling of retinal glial cells. *Neurochem. Res.*, **35**, 522–530.

Niu, Y., Zhao, Y., Gao, Y., Zhou, Z., Wang, H., & Yuan, C. (2004) Therapeutic effect of bFGF on retina ischemia-reperfusion injury. *Chin. Med. J. (Engl).*, **117**, 252–257.

O'Driscoll, C., Wallace, D., & Cotter, T.G. (2007) bFGF promotes photoreceptor cell survival in vitro by PKA-mediated inactivation of glycogen synthase kinase 3beta and CREB-dependent Bcl-2 up-regulation. *J. Neurochem.*, **103**, 860–870.

O'Driscoll, C., O'Connor, J., O'Brien, C.J., & Cotter, T.G. (2008) Basic fibroblast growth factor-induced protection from light damage in the mouse retina in vivo. *J. Neurochem.*, **105**, 524–536.

Pang, J.-J., Boye, S.L., Kumar, A., Dinculescu, A., Deng, W., Li, J., Li, Q., Rani, A., Foster, T.C., Chang, B., Hawes, N.L., Boatright, J.H., & Hauswirth, W.W. (2008) AAV-mediated gene therapy for retinal degeneration in the rd10 mouse containing a recessive PDEbeta mutation. *Invest. Ophthalmol. Vis. Sci.*, **49**, 4278–4283.

Pinto, M.C.X., Tonelli, F.M.P., Vieira, A.L.G., Kihara, A.H., Ulrich, H., & Resende, R.R. (2016) Studying complex system: calcium oscillations as attractor of cell differentiation. *Integr. Biol. (Camb).*, **8**, 130–148.

Puro, D.G. & Mano, T. (1991) Modulation of calcium channels in human retinal glial cells by basic fibroblast growth factor: a possible role in retinal pathobiology. *J. Neurosci.*, **11**, 1873–1880.

Qin, Y., Chen, Z., Han, X., Wu, H., Yu, Y., Wu, J., Liu, S., & Hou, Y. (2015) Progesterone attenuates Aβ25-35-induced neuronal toxicity via JNK inactivation and progesterone receptor membrane component 1-dependent inhibition of mitochondrial apoptotic pathway. *J. Steroid Biochem. Mol. Biol.*, **154**, 302–311.

Rodríguez-Muela, N., Hernández-Pinto, a M., Serrano-Puebla, a, García-Ledo, L., Latorre, S.H., de la Rosa, E.J., & Boya, P. (2014) Lysosomal membrane permeabilization and autophagy blockade contribute to photoreceptor cell death in a mouse model of retinitis pigmentosa. *Cell*

Death Differ., **22**, 476–487.

Rosenthal, R., Malek, G., Salomon, N., Peill-Meininghaus, M., Coeppicus, L., Wohlleben, H., Wimmers, S., Bowes Rickman, C., & Strauss, O. (2005) The fibroblast growth factor receptors, FGFR-1 and FGFR-2, mediate two independent signalling pathways in human retinal pigment epithelial cells. *Biochem. Biophys. Res. Commun.*, **337**, 241–247.

Samadi, A., Carlson, C.G., Gueorguiev, A., & Cenedella, R.J. (2002) Rapid, non-genomic actions of progesterone and estradiol on steady-state calcium and resting calcium influx in lens epithelial cells. *Pflugers Arch.*, **444**, 700–709.

Samardzija, M., Wariwoda, H., Imsand, C., Huber, P., Heynen, S.R., Gubler, A., & Grimm, C. (2012) Activation of survival pathways in the degenerating retina of rd10 mice. *Exp. Eye Res.*, **99**, 17–26.

Sancho-Pelluz, J., Arango-Gonzalez, B., Kustermann, S., Romero, F.J., van Veen, T., Zrenner, E., Ekström, P., & Paquet-Durand, F. (2008) Photoreceptor Cell Death Mechanisms in Inherited Retinal Degeneration. *Mol. Neurobiol.*, **38**, 253–269.

Schmittgen, T.D. & Livak, K.J. (2008) Analyzing real-time PCR data by the comparative C(T) method. *Nat. Protoc.*, **3**, 1101–1108.

Sharma, A.K. & Rohrer, B. (2004) Calcium-induced calpain mediates apoptosis via caspase-3 in a mouse photoreceptor cell line. *J. Biol. Chem.*, **279**, 35564–35572.

Swiatek-De Lange, S., Stampfl, A., & Hauck, S. (2007) Membrane initiated effects of progesterone on calcium dependent signaling and activation of VEGF gene expression in retinal glial cells. *Glia*, **1073**, 1061–1073.

Wójcik-piotrowicz, K., Kaszuba-zwoińska, J., Rokita, E., & Thor, P. (2016) Cell viability modulation through changes of Ca2+-dependent signalling pathways. *Prog. Biophys. Mol. Biol.*, 1–9.

Wyse-Jackson, A.C. & Cotter, T.G. (2016) The synthetic progesterone "Norgestrel" is neuroprotective in stressed photoreceptor-like cells and retinal explants, mediating its effects via basic fibroblast growth factor, protein kinase A and glycogen synthase kinase 3β signalling. *Eur. J. Neurosci.*, **43**, 899–911.

Wyse-Jackson, A.C., Roche, S.L., Byrne, A.M., Ruiz-Lopez, A.M., & Cotter, T.G. (2016) Progesterone Receptor Signalling in Retinal Photoreceptor Neuroprotection. *J. Neurochem.*, **136**, 63–77.

Yang, F., Liu, Y., Tu, J., Wan, J., Zhang, J., Wu, B., Chen, S., Zhou, J., Mu, Y., & Wang, L. (2014) Activated astrocytes enhance the dopaminergic differentiation of stem cells and promote brain repair through bFGF. *Nat. Commun.*, **5**, 5627.

Yousuf, S., Atif, F., Sayeed, I., Tang, H., & Stein, D.G. (2014) Progesterone in transient ischemic stroke: a dose-response study. *Psychopharmacology (Berl).*, **231**, 3313–3323.

Zamburlin, P., Ruffinatti, F.A., Gilardino, A., Farcito, S., Parrini, M., & Lovisolo, D. (2013) Calcium signals and FGF-2 induced neurite growth in cultured parasympathetic neurons: spatial localization and mechanisms of activation. *Pflügers Arch. Eur. J. Physiol.*, **465**, 1355–1370.

Zucchi, R. & Ronca-Testoni, S. (1997) The sarcoplasmic reticulum Ca2+ channel/ryanodine receptor: modulation by endogenous effectors, drugs and disease states. *Pharmacol. Rev.*, **49**, 1–51.

Table 1. List of Qiagen QuantiTect Primer primers used throughout this study

Gene	Qiagen Primer	Product Size (bp)	RefSeq ID#
Actin	QT00095242	149	NM_007393
GAPDH	QT01658692	144	NM_008084
HPRT	QT00166768	168	NM_013556
bFGF	QT00128135	138	NM_008006

Figure Legends

Figure 1. Schematic representation of the intracellular signalling events regulated by the synthetic progesterone Norgestrel. **(A)** Graphical abstract: the diagram illustrates only the pathways reported in this study to be affected by Norgestrel signalling. We propose that it is this pathway through which Norgestrel exerts its neuroprotective effects in photoreceptor cells *in vitro*. **(B)** Experiments carried out throughout the course of this study have been highlighted over the reported pathway and the relevant figure stated.

Figure 2. Norgestrel triggers cytosolic calcium influx in healthy 661W cone photoreceptors cells over three hours. **(A)** Healthy 661W cells were gated. **(B)** Calcium specific indicator, Fluo-4 AM was used to detect changes in intracellular calcium. Healthy 661Ws were treated with 20μM Norgestrel or equivalent DMSO control over 3 and 24 h. Fluo-4 AM fluorescence of the gated cell populations was measured using flow cytometry and plotted on a histogram. Y-axis represents cell counts, x-axis measures the level of fluorescence. A shift to the right along the x-axis represents an increase in Fluo-4 AM fluorescence and hence intracellular calcium level. **(B) (i)** Histograms show untreated cells (grey) compared to a timed DMSO control (black) or Norgestrel-treated cells (blue). **(B) (ii)** Relative geomean of all treatments was determined and graphed compared to untreated cells (t-test comparing individual Norgestrel treatments to their timed DMSO control, ****$p<0.001$).

Figure 3. Serum starvation triggers cytosolic calcium influx in 661W cone photoreceptors cells over three hours. (A) 661W cells were serum starved over 24 h and Fluo-4 AM fluorescence was measured. **(A) (i)** Histograms show untreated control (grey) compared to a timed serum starved sample (black). **(A) (ii)** Relative geomean of all treatments was determined and graphed compared to untreated cells (ANOVA followed by Dunnett's multiple comparisons test, comparing all time points to the untreated control, ****p<0.001). Figures are representative of three independent experiments, repeated in triplicate. All results are presented as mean ± SEM. Asterisks indicate significant difference. **(B, C)** Live, representative confocal microscopic images of 661W cells following serum starvation for the indicated times. **(B)** Serum starvation of 661W cells causes an initial retraction of cellular processes. Cells begin to settle again, extending spindle like processes out after 2 h serum starvation. **(C)** Live imaging of intracellular calcium (Fluo-4 AM; green) in serum starved 661W cells compared to untreated control. Scale bars 30 μm. **(D)** Changes in cell viability over 24h was measured by the MTS assay and graphed as a percentage of 100% viable untreated cell control (n=4) (ANOVA followed by Dunnett's multiple comparisons test comparing all time points to the untreated control, **p<0.01, ****p<0.001).

Figure 4. Norgestrel causes an increase in cytosolic calcium in stressed 661W cells over 24 hours. **(A)** 661W cells were serum starved **over 24 h** in the absence or presence of 20 μM Norgestrel. An increase in intracellular calcium levels in response to Norgestrel was verified by flow cytometry using calcium specific indicator, Fluo-4 AM. Results were plotted on a histogram: Y-axis represents cell counts, x-axis measures the level of fluorescence. A shift to the right along the x-axis represents an increase in Fluo-4 AM fluorescence and hence intracellular calcium level. Histograms show untreated cells (grey) compared to serum starved, timed DMSO (black) or Norgestrel (blue) treated cells. **(B)** Representative live confocal microscopic imaging of intracellular calcium (Fluo-4 AM; green) in serum starved 661W cells treated over 24 h with 20 μM Norgestrel or DMSO control. Scale bars 30μm. **(C)** Relative geomean of all treatments was determined and graphed compared to untreated cells (t-test comparing individual Norgestrel treatments to their timed DMSO control, *p<0.05, ****p<0.001). Results are presented as mean ± SEM. Asterisks indicate significant difference. Figures are representative of three independent experiments, repeated in triplicate.

Figure 5. Norgestrel acts through PGRMC1 to induce an increase in cytosolic calcium. **(A)** PGRMC1 specific inhibitor AG205 causes a dose dependent increase in intracellular calcium in stressed 661W cells, as measured by flow cytometry using calcium specific indicator, Fluo-4 AM. **(B)** 661W cells were serum starved over 24 h and treated with 20 μM Norgestrel or equivalent DMSO control in the absence or presence of 1 μM AG205. Percentage cell death was assayed (n=4). AG205 attenuates Norgestrel-induced cell survival (ANOVA followed by Tukey's multiple comparisons test comparing all treatments, ****p<0.001). **(C, D)** 661W cells were serum starved over 3 h and treated with 20 μM Norgestrel and/or 1 μM AG205. AG205 treatment prevented a Norgestrel-induced increase in intracellular calcium, as determined by flow cytometry using calcium specific indicator, Fluo-4 AM. Results were plotted on a histogram: Y-axis represents cell counts, x-axis measures the level of fluorescence. A shift to the right along the x-axis represents an increase in Fluo-4 AM fluorescence and hence intracellular calcium level. **(D)** Relative geomean of all treatments was determined and graphed compared to untreated cells (ANOVA followed by Dunnett's multiple comparison's test comparing all treatments to their individual timed DMSO serum starved control,

****p<0.001). Results are presented as mean ± SEM. Asterisks indicate significant difference. Figures are representative of three independent experiments, repeated in triplicate.

Figure 6. Norgestrel activates PGRMC1 to induce an upregulation of bFGF, causing a subsequent influx of cytosolic calcium. **(A)** 661W cells were serum starved for 1 h in the presence or absence of 20 μM Norgestrel and/or 1 μM PGRMC1 specific inhibitor, AG205. Rt-qPCR analysis detected a significant increase in bFGF mRNA levels over 1 h in response to Norgestrel, relative to timed DMSO control. This increase was abrogated through treatment with 1 μM AG205 (ANOVA followed by Tukey's multiple comparisons test comparing all treatments, ns=no significance, *p<0.05). **(B – D)** 661W cells were transfected with siRNA against bFGF or non-targeting scrambled control (Scrambled) for 48 hours before treatment. **(B)** Detection of bFGF mRNA levels by rt-qPCR and immunofluorescence. **(B) (i)** Relative levels of bFGF were measured compared to scrambled siRNA control, confirming ~70% knock down at the mRNA level. (B) (ii) Immunofluorescence imaging of bFGF siRNA treated 661Ws confirmed bFGF protein knock down compared to scrambled control. Scale bars 30 μM. **(C)** Transfected cells were serum starved for 1 h in the presence of 20 μM Norgestrel or equivalent DMSO control and intracellular calcium levels were measured by flow cytometry using calcium specific indicator, Fluo-4 AM. **(C) (i)** Results were plotted on a histogram: Y-axis represents cell counts, x-axis measures the level of fluorescence. A shift to the right along the x-axis represents an increase in Fluo-4 AM fluorescence and hence intracellular calcium level. **(C) (ii)** Relative geomean of all treatments was determined and graphed compared to untreated cells (t-test comparing individual Norgestrel treatment to equivalent serum starved scrambled or siRNA DMSO control, ns=no significance, ****p<0.001). Results are presented as mean ± SEM. Asterisks indicate significant difference. Figures are representative of three independent experiments, repeated in triplicate.

Figure 7. Extracellular calcium influx is necessary for Norgestrel-induced neuroprotection. **(A)** 661W cells were serum starved for 1 h and treated with 0.5 mM EGTA (extracellular calcium chelators) and/or 1 μM dantrolene (antagonist of IP3/ryanodine receptors) in presence or absence of 20 μM Norgestrel. Intracellular calcium levels were measured by flow cytometry using calcium specific indicator, Fluo-4 AM. **(A) (i)** Results were plotted on a histogram: Y-axis represents cell counts, x-axis measures the level of fluorescence. A shift to the right along the x-axis represents an increase in Fluo-4 AM fluorescence and hence intracellular calcium level. **(A) (ii)** Relative geomean of all treatments was determined and graphed compared to untreated cells (t-test comparing all individual Norgestrel treatments to specific pre-treated DMSO control, ****p<0.001). **(B) (i)** Non-stressed 661W cells were treated with increasing concentrations of L-type calcium channel blocker verapamil (10 – 100 μM) for 1 hour and measured by flow cytometry for changes in intracellular calcium using calcium specific indicator, Fluo-4 AM. Relative geomean of all treatments was compared to untreated cells (ANOVA followed by Dunnet's multiple comparisons test comparing all treatments to untreated cells, ***p<0.005, ****p<0.001). **(B) (ii)** 661W cells were serum starved for 1 h and treated with 50 μM verapamil in presence of 20 μM Norgestrel or equivalent DMSO control. Intracellular calcium levels were measured by flow cytometry using calcium specific indicator, Fluo-4 AM. Relative geomean of all treatments was determined and graphed compared to untreated cells (t-test comparing all individual Norgestrel treatments to specific pre-treated DMSO control, ns = no significance, ****p<0.001). **(C)** 661W cells were serum starved

for 24 h and treated with 20 μM Norgestrel or equivalent DMSO control in the absence or presence of 0.5 mM EGTA. Percentage cell death was assayed (n=4). EGTA attenuates Norgestrel-induced cell survival (ANOVA followed by Tukey's multiple comparisons test, ns=no significance, ****p<0.001). Results are presented as mean ± SEM. Asterisks indicate significant difference. All figures are representative of three independent experiments, repeated in triplicate.

(A) Graphical Abstract

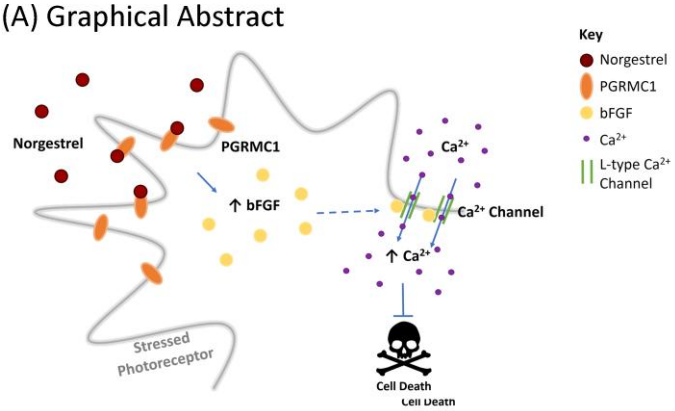

(B) Experimental Schematic